

Article

## ***In Situ* and *Ex Situ* Syntheses of Magnetic Liquid Crystalline Materials: A Comparison**

Ophelie Riou <sup>1,2</sup>, Lacramiora Zadoina <sup>1,2</sup>, Barbara Lonetti <sup>1,\*</sup>, Katerina Soulantika <sup>2</sup>, Anne-Françoise Mingotaud <sup>1</sup>, Marc Respaud <sup>2</sup>, Bruno Chaudret <sup>2</sup> and Monique Mauzac <sup>1</sup>

<sup>1</sup> Laboratoire IMRCP (Interactions Moléculaires et Réactivité Chimique et Photochimique), Université de Toulouse and CNRS, UMR 5623, 118 route de Narbonne, 31062 Toulouse, France; E-Mails: riou@chimie.ups-tlse.fr (O.R.); zadoina@gmail.com (L.Z.); afmingo@chimie.ups-tlse.fr (A.-F.M.); mauzac@chimie.ups-tlse.fr (M.M.)

<sup>2</sup> Université de Toulouse; INSA, UPS, LPCNO, 135 avenue de Rangueil, 31077 Toulouse, France; and CNRS; LPCNO, 31077 Toulouse, France; E-Mails: katerina.soulantika@insa-toulouse.fr (K.S.); marc.respaud@insa-toulouse.fr (M.R.); bruno.chaudret@insa-toulouse.fr (B.C.)

\* Author to whom correspondence should be addressed; E-Mail: lonetti@chimie.ups-tlse.fr; Tel.: +33-561-556-272; Fax: +33-561-558-155.

Received: 19 December 2011; in revised form: 30 January 2012 / Accepted: 31 January 2012 /

Published: 10 February 2012

---

**Abstract:** Magnetic hybrid liquid crystalline composites have been obtained either by thermal decomposition of a cobalt precursor in a solution containing a liquid crystal polymer or by dispersing preformed cobalt nanorods in a liquid crystal polymer matrix. The final materials are all mesomorphous and ferromagnetic. Their magnetic characteristics are compared as a function of the synthesis method.

**Keywords:** polymer magnets; metallic nanoparticles; liquid crystal polymer; magnetic hybrid; artificial muscle

---

### **1. Introduction**

The field of stimuli responsive materials is huge; it concerns several domains such as medicine, pharmaceuticals, biotechnology, but also nanotechnology and engineering. Among these materials, shape-memory polymers are an emerging class of polymers with applications spanning over various

areas of everyday life [1]. Shape-memory polymers are elastic polymer networks equipped with suitable stimuli-sensitive switches.

The thermotropic elastomers display shape-memory properties triggered by the thermal transition of the liquid-crystalline domains [2–4]. This phenomenon occurs from the strong coupling between the orientational order of the liquid crystalline units integrated in the polymer matrix and the rubber elasticity of the polymer network. During shape-changing, the mesogenic groups act as a switch and the molecular movement of the single liquid crystals is responsible for a macroscopic movement. Macroscopically oriented liquid crystal elastomers exhibit large and reversible deformations when they undergo a liquid crystal to isotropic phase transition.

Temperature is the most usually employed stimulus for actuating liquid crystalline elastomers but light or electric fields have been also considered [5,6]. Liquid crystalline elastomers containing an inorganic material may offer new original solutions for the development of other stimuli-responsive materials, making use of the intrinsic properties of the inorganic nuclei. For instance, dispersing magnetic particles within these elastomers could provide shape-changing materials by means of an applied magnetic field during the isotropic/mesogenic phase transition. Moreover, the use of magnetic particles should enhance the magneto-orientational response of liquid crystals, as first proposed by Brochard and de Gennes in the 1970s [7] then experimentally tested some years later. The as obtained doped nematic liquid crystals could be oriented by a magnetic field intensity  $10^3$  times smaller than usual [8,9].

In the literature, magnetic nanoparticles have been mixed with various low molecular weight lyotropic or thermotropic liquid crystals and the effect of particle size and concentration of the particles on the mesomorphous properties was mostly investigated [10,11]. Only a few three-dimensional liquid crystalline networks [12–14] including iron oxide nanoparticles were described and reported to exhibit interesting magnetic properties. For example Song *et al.* covalently bonded dopamine anchored ferrite nanoparticles on a liquid crystal elastomer. The composite showed superparamagnetic behavior at 300 K [12]. In another work, spherical magnetic  $\text{Fe}_2\text{O}_3$  nanoparticles were introduced into an oriented liquid crystal elastomer in which a nematic/isotropic transition is produced by a temperature increase due to particles thermal motion induced by an alternating magnetic field [13]. Finally, spherical iron oxide particles were used as cross-linking agents for linear mesogenic oligomers [14]. A smectic phase was induced at room temperature and the magnetic properties appeared almost unchanged compared to those of the pure particles.

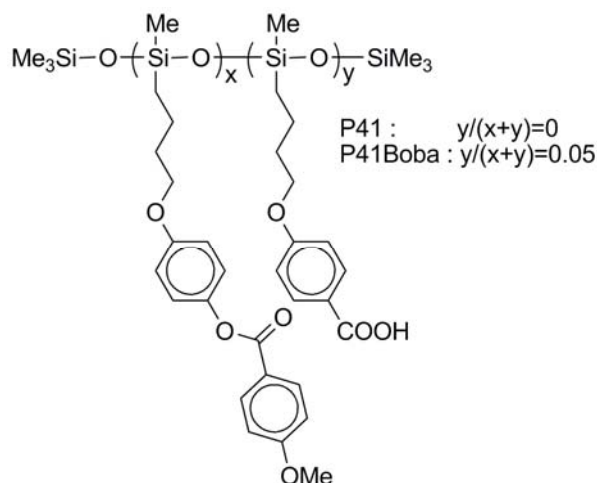
In a previous report [15], we presented a new composite obtained by dispersing preformed metallic cobalt nanorods in a liquid crystal polymer. In another work [16] we presented the results obtained by the *in situ* synthesis of Co nanoparticles in the same liquid crystal polymer matrix. In both cases, the liquid crystal order of the polymer was maintained and the magnetic properties of the particles were improved thanks to the interaction with the liquid crystalline matrix. The aim of the present work is to compare, the mesomorphous and magnetic properties of the hybrid materials obtained by these approaches. Finally, a liquid crystalline elastomer is then described from the most efficient polymer composite.

## 2. Results and Discussion

In this work we compare two methods for the fabrication of a new material where cobalt nanoparticles are dispersed in a liquid crystal polymer. The cobalt particles can be: (i) synthesized inside the liquid crystalline polymer (*in situ*) or (ii) pre-formed and then dispersed inside the same liquid crystalline polymer (*ex situ*).

The liquid crystal polymer (LCP) of choice is represented in Figure 1. It was synthesized following previously described procedures [17]. It is a statistical copolymer composed of a flexible polysiloxane chain and one or two types of mesogenic moieties. Two types of polymers, P41 and P41Boba, were synthesized with different ratios between the mesogenic moieties. Both polymers possess a smectic A ( $S_A$ ) and nematic (N) phase: P41 passes from the  $S_A$  to the N phase at 74 °C and to the isotropic state at 104 °C; in the case of P41Boba 85 °C and 95 °C are respectively the  $S_A$  to N and N to isotropic phases transition temperatures.

**Figure 1.** Structure of the liquid crystalline polymers.



The cobalt precursor, bis(bis(trimethylsilyl)amido)cobalt(II)  $\text{Co}[\text{N}(\text{SiMe}_3)_2]_2$ , was synthesized according to the procedure described by Andersen *et al.* [18]. The cobalt particles were obtained using a procedure similar to that reported before [19], either in an anisole solution (*ex situ* synthesis), or in a toluene solution containing the liquid crystalline polymer (*in situ* synthesis).

### 2.1. In Situ Synthesis of the Magnetic Liquid Crystal Polymer Composites

In the present work, the decomposition of the cobalt precursor was performed in the presence of the P41 or P41Boba liquid crystal polymer at 120 °C in toluene under 3 bar  $\text{H}_2$  pressure and the reaction time was modified between 3 and 48 h. The synthesis already described in the literature [19] uses long chain organic compounds as ligands (usually an acid and an amine) and it has been pointed out that the presence of both acid and amine functions favors anisotropic growth. We aimed at obtaining anisotropic single domain nanoparticles to get large blocking temperature and ferromagnetic at room temperature thanks to their increased shape anisotropy. Since we wanted to explore the consequences of the presence of a liquid crystal polymer on the reaction under all experimental conditions; the effect of only one or the two ligands was also assessed.

It has also to be noted that in the P41Boba the acid ligand is directly linked to the polymer chain. This affects the mobility of this species and consequently the reaction kinetics compared to low molecular weight systems. The synthesis conditions used and the nanoparticles obtained are summarized in Table 1.

**Table 1.** Sample composition, wt% Co, time of reaction, nanoparticle sizes (d is the diameter of spherical nanoparticles and L is the length of the anisotropic ones) and isotropic to nematic transition temperatures changes of the composites as obtained by Polarized Optical Microscopy (POM) are reported in the case of the samples obtained in the *in situ* synthesis.

P41	wt%Co	hours	Nanoparticles size	$\Delta T$
HDA:Co=1	1.5	3	d = 8.0 ± 1.3 nm	-15.5
Boba:Co = 0.16	10	3	d = 8.0 ± 1.5 nm; d = 4 ± 1 nm	-
Boba:Co = 1	1.5	3	d = 8.0 ± 1.5 nm	-35
Boba: HDA:Co = 0.16:0.16:1	10	3	d = 5 ± 1.5	-21
Boba: HDA:Co = 0.16:0.16:1	10	14	d = 17 ± 3 nm; L = 24 ± 5 nm	-43
Boba: HDA:Co = 1:1:1	1.5	3	d = 10 ± 5 nm	-12.5
Boba: HDA:Co = 1:1:1	1.5	24	d = 8 ± 1 nm; d = 4 ± 0.8 nm	-33
<b>P41Boba</b>				
Boba:Co = 1	0.8	48	d = 10 ± 2 nm	0
Boba:Co = 0.65	1.25	48	d = 14 ± 2 nm	-6
Boba:Co = 0.16	4	48	L = 14 ± 2 nm	-14
Boba:HDA:Co = 1:1:1	0.8	17	d = 16 ± 2 nm	-23
Boba:HDA:Co = 0.65:1:1	1.25	17	d = 14 ± 2 nm	-18
Boba:HDA:Co = 0.16:1:1	4	17	d = 5 ± 1 nm; L = 20 ± 7 nm	-6

### 2.1.1. *In Situ* Synthesis of Co Nanoparticles in the Presence of the Liquid Crystal Polymer P41

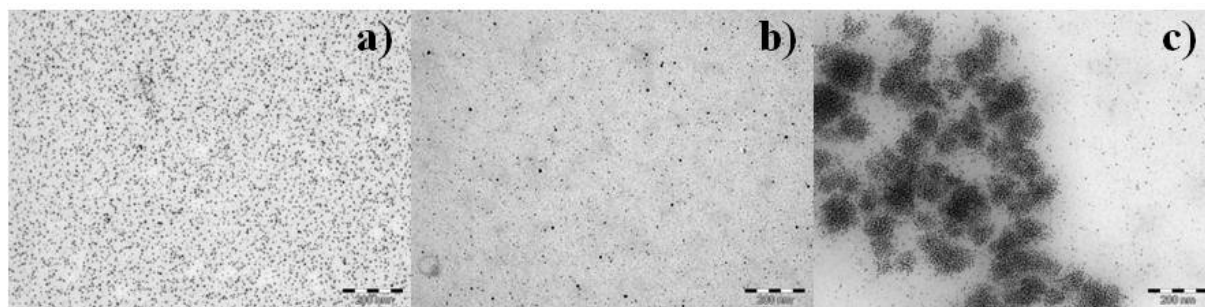
When the Co precursor was decomposed in a toluene solution containing only the liquid crystal polymer P41, very few particles were obtained and almost all of them aggregated.

In order to improve the stabilization of the nanoparticles, we added the 4-(3-butenyloxy)benzoic acid group (Boba) and/or hexadecylamine (HDA) as ligands and we examined the effect of the Boba:Co and HDA:Co ratios on the kinetics of the reaction and on the particles' morphology. Cobalt concentration was varied between 1.5 wt% and 10 wt%, and different molar ratios of Boba:Co and HDA:Co, between 0 and 1, were tested. The reaction time was fixed to 3 hours and the temperature to 120 °C.

In the presence of amine as the only ligand no particles were obtained for low HDA content (ratio equal to 0.16), while 8.0 ± 1.3 nm nanoparticles were obtained for HDA:Co ratio equal to 1 (Figure 2(a)).

On the other hand, when only Boba is present, two populations of 8.0 ± 1.5 nm and 4 ± 1 nm, with the small nanoparticles being the major product, were obtained at low Boba content (Boba:Co equal to 0.16), see Figure 2(b). Mostly 8.0 ± 1.5 nm particles were formed when the acid concentration was increased to a ratio Boba:Co equal to 1 (Figure 2(c)).

**Figure 2.** Co nanoparticles obtained with P41 after 3 h at 120 °C for (a) HDA: Co = 1 (1.5 wt% Co) (b) Boba:Co = 0.16 (10 wt% Co) (c) Boba:Co = 1 (1.5 wt% Co). Scale bars: 200 nm.

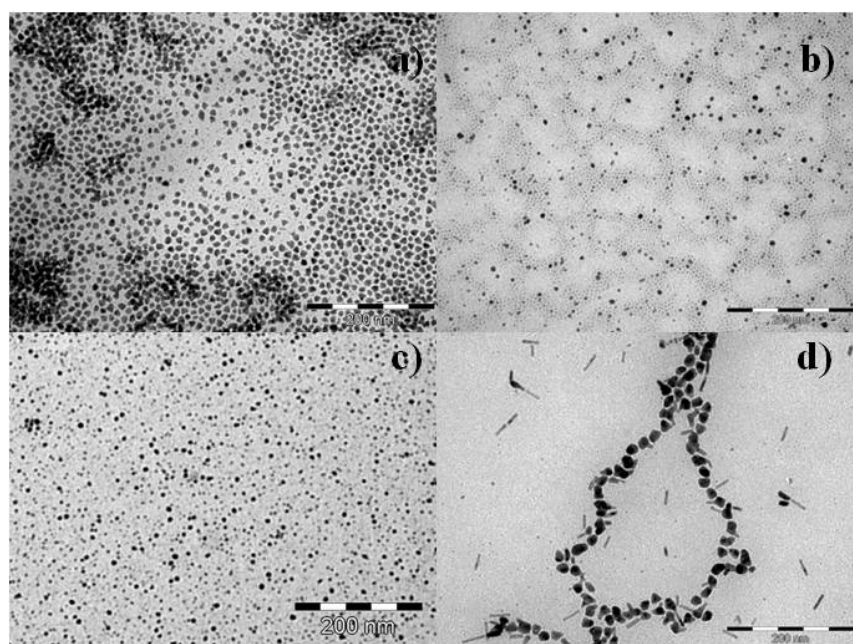


For this last Boba:Co ratio, the stabilization is more effective and larger and more homogeneous nanoparticles are formed.

The addition of only one kind of ligand led to the formation of homogeneous spherical nanoparticles, and since we want to induce some anisotropy we decided to use both ligands as in the case of our previous work in the absence of liquid crystalline molecules [19]. For this purpose, we examined the effect of the addition of both Boba and HDA to the P41 in an equimolar ratio, and the effect of the reaction time was studied.

At 1.5 wt% of cobalt (Boba:HDA:Co = 1:1:1), after 3 h reaction, the precursor decomposition led to the formation of irregular (triangular and spherical) nanoparticles of mean size  $10 \pm 5$  nm (Figure 3(a)). If the reaction was left longer, till 24 h, surprisingly two populations of spherical particles,  $8 \pm 1$  nm and  $4 \pm 0.8$  nm, were formed (Figure 3(b)).

**Figure 3.** Co nanoparticles obtained with P41 in the presence of both Boba and HDA at 120 °C (a) for Boba:HDA:Co = 1:1:1 (1.5wt% Co) after 3 h (b) for Boba:HDA:Co = 1:1:1 (1.5 wt% Co) after 24 h (c) for Boba:HDA:Co = 0.16:0.16:1 (10wt% Co) after 3 h (d) for Boba:HDA:Co = 0.16:0.16:1 (10wt% Co) after 14 h. Scale bars: 200 nm



When the cobalt concentration was increased to 10wt% (Boba:HDA:Co = 0.16:0.16:1),  $5 \pm 1.5$  nm spherical nanoparticles were obtained after 3 h (Figure 3(c)). After 14 hours, larger nanoparticles ( $17 \pm 3$  nm) formed with the tendency to self-organize (Figure 3(d)). Some anisotropic nanoparticles were also observed ( $24 \pm 5$  nm length).

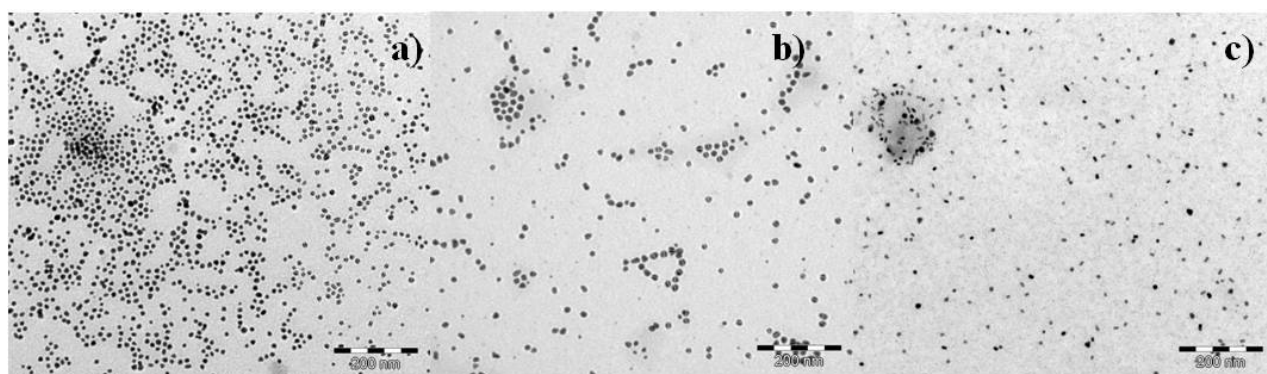
Surprisingly anisotropic nanocrystals were obtained for a low ligands to Co ratio (Boba:HDA:Co = 0.16:0.16:1) after 14 hours. It is possible that at longer times higher Co as well as of the nanoparticles concentration in the medium enables the growth or coalescence of smaller particles along certain axes.

### 2.1.2. *In Situ* Synthesis of Co Nanoparticles in the Presence of the Liquid Crystal Polymer P41Boba

The effect of acid immobilization on the polymeric chain is worth to be examined. For this, P41 Boba, in which the acid moiety is part of the polymer chain, was used. In this case the acid diffusion in the solution is inhibited. In this series of experiments, we examined the effect of the Boba:Co ratio on the nanoparticles morphology.

The reaction time was fixed to 48 hours: we obtained spherical monodispersed nanoparticles of  $10 \pm 2$  nm and  $14 \pm 2$  nm in the case of Boba:Co ratios of 1 and 0.65 respectively (Figure 4(a,b)) [16]. In the case of Boba:Co ratio of 0.16, more rectangular shape nanoparticles  $14 \pm 2$  nm mean length (Figure 4(c)) were obtained [16]. Increasing the Co content, from 0.8 wt% (Boba:Co = 1) to 5 wt% (Boba:Co = 0.16), larger particles were formed and, for strong Co excess, the coalescence of smaller particles was probably favored

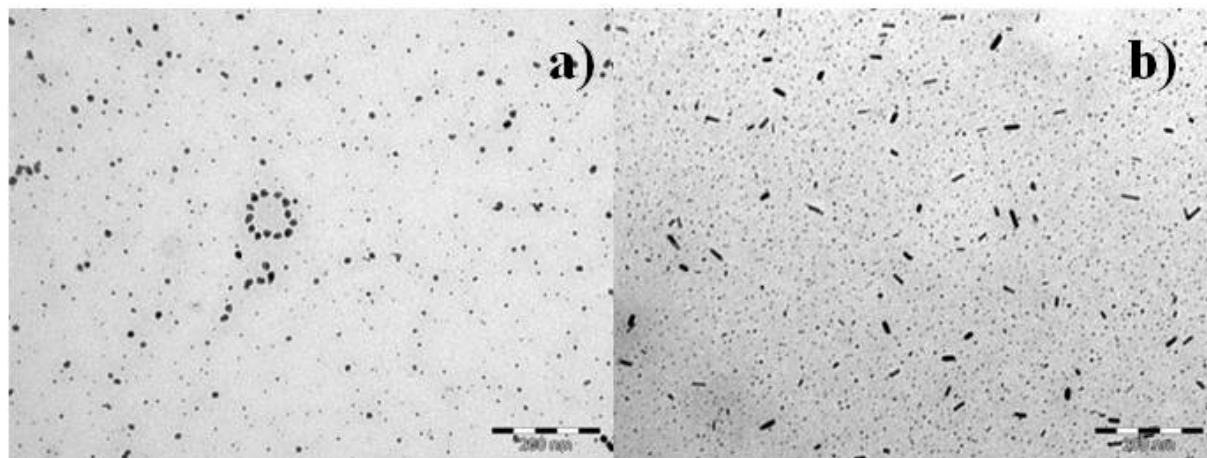
**Figure 4.** Co nanoparticles obtained with P41Boba polymer after 48 h at 120 °C for (a) Boba:Co = 1 (0.8 wt% Co) (b) Boba:Co = 0.65 (1.25 wt% Co) (c) Boba:Co = 0.16 (4 wt% Co). Scale bars: 200 nm.



As in the case of P41 mixed with Boba monomer, the presence of an acid moiety alone is not enough to induce an anisotropic growth. We therefore added the amine ligand in order to evaluate the possibility to form anisotropic nanoparticles. The reaction time was fixed to 17 hours and the ratio between the components was varied.

Spherical nanoparticles were observed for Boba:HDA:Co=1:1:1 and Boba:HDA:Co=0.65:1:1 (Figure 5(a)), respectively of  $16 \pm 2$  nm and  $14 \pm 2$  nm. When the Boba content was reduced to Boba:HDA:Co=0.16:1:1, nanorods with a mean length of  $20 \pm 7$  nm and  $7 \pm 1$  nm diameter became predominant. Some small particles of  $5 \pm 1$  nm diameter were also present [16].

**Figure 5.** Co nanoparticles obtained with P41Boba polymer after 17 h at 120 °C for (a) Boba:HDA:Co = 0.65:1:1 (1.25 wt% Co); (b) Boba:HDA:Co = 0.16:1:1 (4 wt% Co). Scale bars: 200 nm.



Both for P41 and P41Boba, nanorods were obtained, always mixed with spherical nanoparticles, when the Boba content was low (0.16). This result is different from what was observed when no polymer was present in the medium [19] in which equimolar ratios of lauric acid, HDA and Co monomer were used. We can attribute this difference to the fact that the polymer matrix slows down the diffusion of the molecules, but also to the fact that the acid function is immobilized on the polymers chain. The consequence would be a lack of homogeneity of the cobalt species concentration in solution influencing the two steps of the nanoparticles formation (nucleation and growth). An in depth understanding of the formation mechanism of the nanorods, which may explain all the experimental observations both in the presence and in the absence of polymer, is not yet possible.

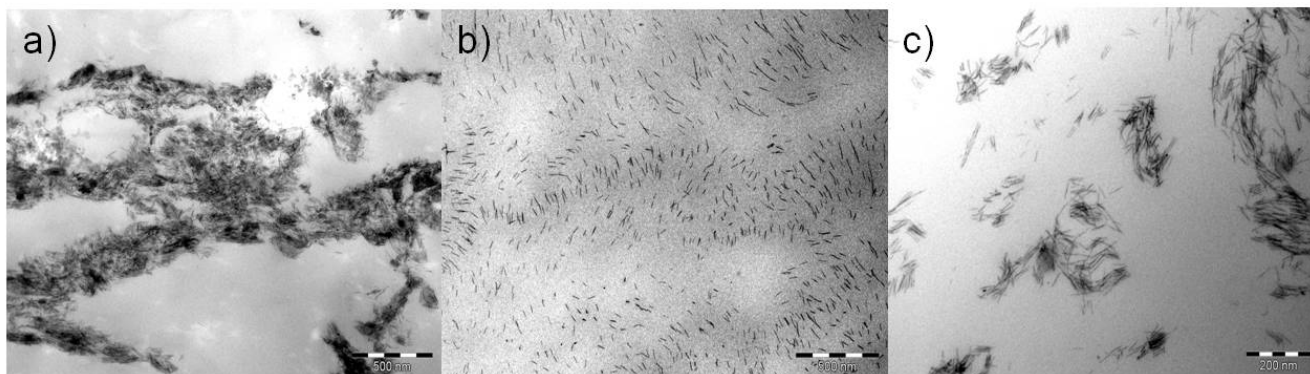
## 2.2. Ex Situ Synthesis of the Magnetic Liquid Crystal Polymer Composites

The cobalt nanorods were synthesized from an organometallic precursor according to a well established protocol [19] which provides monocrystalline metallic nanorods of 56 nm mean length and 5.5 nm diameter. The nanoparticles are partially covered by a small quantity of ligands (10 wt% with respect to cobalt) after washing them repeatedly. Magnetization measurements evidence a spontaneous magnetization similar to the bulk one. The cobalt nanorods were mixed with the two different liquid crystal polymers, P41 and P41Boba, at two different weight percentages, 1 wt% and 4 wt%. However a good dispersion of the nanorods inside the polymer matrix turned out to be a delicate point, since because of their magnetic character they have a strong tendency to aggregate. Sonication is essential before and after mixing nanorods and polymer solutions. After dispersion no sedimentation of the particles was observed for at least ten months.

Figure 6 reports transmission electron microscopy (TEM) images obtained from different samples after microtomy. They are representative of the possible scenarios of the dispersion.

By efficient sonication we are able to avoid the presence of very dense large areas like in Figure 6(a) which harm the final properties of the composite. On the other hand some denser zones like in Figure 6(c) are difficult to avoid as they arise from the strong magnetic interactions between the nanorods.

**Figure 6.** TEM micrographs of the 4 wt% cobalt nanorods embedded in the polymer matrix P41 (a) and (b) Scale bar: 500 nm (c) Scale bar: 200 nm.



By comparing the two different ways of producing the composites, we can conclude that with the *in situ* procedure, it was not possible to selectively form nanorods.

Therefore, in order to investigate the effect of particles size and shape on the composite's properties the *ex situ* procedure appears more adequate.

### 2.3. Mesomorphic Behavior of the Liquid Crystal Polymer Composites

The thermal transitions of the composites obtained by *in situ* synthesis are summarized in Table 1. In all cases the final doped polymer preserved its mesomorphic properties. The liquid crystal phase is destabilized by 6 to 43 degrees due to the presence of the nanoparticles, but no apparent correlation between the Co content or nanoparticles size and the mesomorphic character could be established.

The thermal transitions of the composites realized by *ex situ* synthesis are presented in Table 2. A slight increase of the transition temperature can be observed for all samples with the exception of P41Boba mixed with 4 wt% nanorods. This stabilization of the nematic phase corresponds to slightly lower transition enthalpies. This is not straightforward to explain, however it does not seem to be connected to the oxidation state of the particles in the composite since the transition temperatures remains unchanged if the sample is left exposed to the air during three months. Earlier studies have demonstrated a destabilization of the mesophases in physical mixtures of liquid crystal and inorganic nanoparticles, which was attributed to chemisorption effects [20]. On the other hand, a recent example showed that fluxional ligands can provide a certain degree of freedom which allows the LC to preferentially organize itself around the nanoparticles and to improve the LC properties [21].

**Table 2.** Isotropic to nematic transition temperature ( $\Delta T$ ) and enthalpic ( $\Delta H$ ) changes of the different composites prepared by *ex situ* synthesis as obtained by Differential Scanning Calorimetry (DSC). The nanorods length in the samples is 56 nm.

	$\Delta T$ [°C]	$\Delta H$ (J/g)
<b>P41 + 1 wt% Co</b>	1.3	−0.09
<b>P41 + 4 wt% Co</b>	3.6	−0.23
<b>P41Boba + 1 wt% Co</b>	1.3	−0.29
<b>P41Boba + 4 wt% Co</b>	−0.4	−0.38

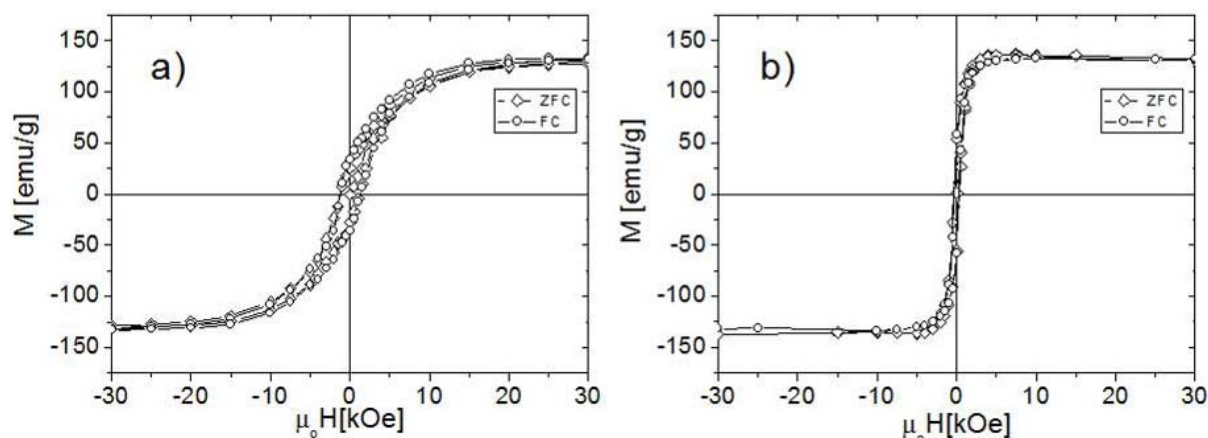
If we compare the two ways of synthesis, all the obtained composites maintain the liquid crystal properties but with a modification of the clearing temperature, however in opposite ways. Since the polymers and the chemical nature of the nanoparticles are the same, a possible explanation could be the different nanoparticle geometry (spherical *vs.* anisotropic nanoparticles), or the presence of by-products acting as an impurity and lowering the liquid crystal stability in the case of the *in situ* synthesis.

#### 2.4. Magnetic Properties of the Liquid Crystal Polymer Composites

The magnetic properties of the different composites were compared through magnetisation measurements with a superconducting quantum interference device (SQUID).

Figure 7 reports typical ferromagnetic hysteresis loops measured for samples containing spherical nanoparticles of  $d = 14 \pm 2$  nm (Boba:HDA:Co = 0.65:1:1, 1.25 wt% Co) and  $d = 10 \pm 2$  nm (Boba:Co = 1, 0.8 wt% Co) obtained from *in situ* synthesis in the presence of P41Boba polymer.

**Figure 7.** Hysteresis loops after Zero field Cooling (ZFC) and Field Cooling (FC,  $H = 5$  T) (a) at 2 K relative to the sample obtained *in situ* with Boba:HDA:Co = 0.65:1:1 ( $d = 14 \pm 2$  nm, Figure 5(a)) (b) at 300 K relative to the sample obtained *in situ* with Boba:Co = 1 ( $d = 10 \pm 2$  nm, Figure 4(a)).

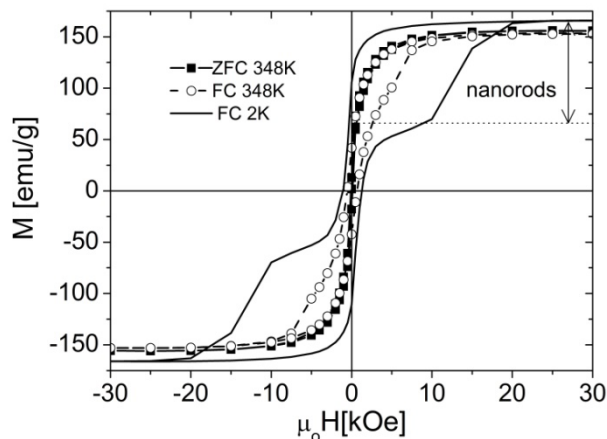


The cycles were registered at 2K and 300K by sweeping the magnetic field between  $H = 5$  T and  $H = -5$  T, after zero field cooling (ZFC) and field cooling from 400 K with a magnetic field of 5 T (FC). The coercive field is 1.2 kOe for the biggest Co nanoparticles at low temperature 2K. It decreases upon increasing the temperature as expected for single domain superparamagnetic objects. Even for the smallest nanoparticles, a coercive field is still measured in the range of 0.4 kOe at 300 K.

Figure 8 shows the SQUID measurements relative to the polymer composite obtained *in situ* containing cobalt nanorods of about 20 nm length and spherical particles of 5 nm diameter (Figure 5(b)).

The measurements were carried out after heating the sample at 367 K (isotropic state) during 10 min in order to erase any organization of the medium and cooling it down to 348 K in the absence of any magnetic field (nematic state) and in the presence of a 3T magnetic field at 348 K and 2 K (glassy state).

**Figure 8.** Hysteresis loops at 348 K after Zero field Cooling (ZFC) and at 348 K and 2 K after Field Cooling (FC,  $H = 3$  T) for the sample obtained *in situ* with Boba:HDA:Co = 0.16:1:1 (sample showed in Figure 5(b)). The nanorods contribution to the total magnetization is indicated by an arrow.

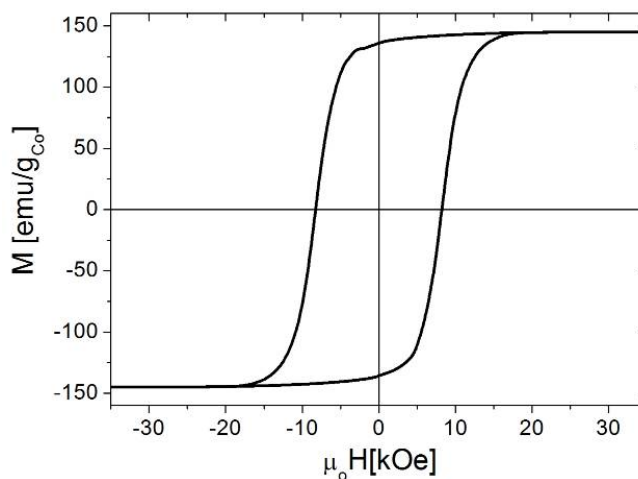


At 2K we observe a reversal of the magnetization in two steps: the first step at weak magnetic fields can be attributed to the spherical nanoparticles (1.3 kOe) while the one at higher fields to the nanorods (10 kOe). The contribution of the nanorods (100.2 emu/g) to the total magnetization (331.6 emu/g) allows us to have a rough estimation of the nanorods content, evaluated to 30%.

When the sample was cooled down to the nematic state (348 K) in the presence of a high magnetic field (3 T) the liquid crystal groups were expected to be oriented: the coercive field of oriented sample was six times larger than the one of the non-oriented one.

Figure 9 reports a typical hysteresis loop relative to a composite P41Boba with 1 wt% Co obtained *ex situ* and registered at 300 K after heating the sample up to the isotropic state (400 K) and cooling it down in the presence of a 5 T magnetic field to its smectic A state.

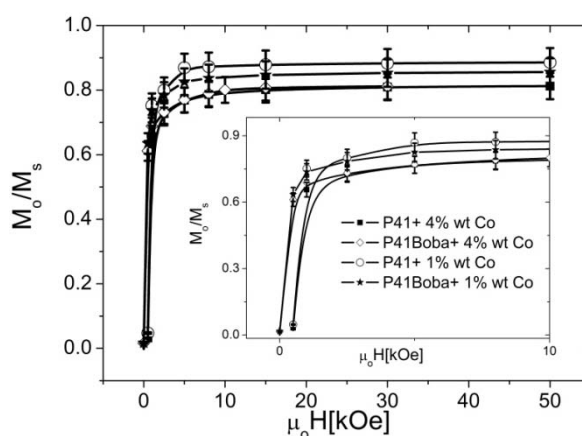
**Figure 9.** Typical hysteresis loop of a P41Boba +1 wt% Co composite at 300K Before the measurement the sample has been heated up during 10 min in the isotropic phase (400 K) in order to erase any possible magnetic history effect, then it has been cooled down in the presence of a 5T magnetic field.



We observe in Figure 9 that the cycle is almost square shaped: the coercive field is 8.2 kOe and the remanence ratio is 0.94. As we already observed in the case of longer nanorods [15], the thermal treatment has considerably improved the nanorods orientation.

In order to determine the minimum field necessary to orientate the nanorods, the sample was heated up in the isotropic phase and cooled down to room temperature under different magnetic fields (from 50 mT to 5 T). The magnetization of the sample after the treatment was measured and compared with the magnetization at saturation where we consider that all the nanorods are oriented. The curves are shown in Figure 10. These are quite steep at low magnetic fields and more than 50% of nanorods are oriented already at 50 mT and at 500 mT the  $M_0/M_s$  value corresponding to a maximum degree of orientation is achieved. Even better orientation can be observed for lower Co concentration. This is probably due to the lower extent of aggregation of the nanorods in these samples. No apparent difference can be observed between the two polymers. The Boba content in the P41Boba polymer is probably too low to appreciate the effect of the interaction with the nanorods. It must be noted that the curves in the presence of the liquid crystalline polymer are steeper than in the case of an inert matrix (tetracosane) due to some cooperative effects between the mesogen groups and the nanorods [15].

**Figure 10.** Initial magnetization divided by saturation magnetization as a function of the magnetic field applied during cooling from 400 K to 300 K in the case of different samples of P41 and P41Boba containing 1 wt% and 4 wt% Co nanorods.



Both in the case of the *in situ* and *ex situ* synthesis the magnetization at saturation is close to the bulk value of Co ( $163 \text{ emu g}^{-1} \text{ Co}$ ). This confirms the metallic character of Co.

The differences in the magnetic behavior of the composites obtained by the two methods are essentially due to the nanoparticle shape which is practically spherical in the *in situ* method and anisotropic in the *ex situ* synthesis. Compared to composites obtained *in situ*, the *ex situ* ones possess superior ferromagnetic properties as they contain only the nanorods.

*In situ* samples containing only spherical nanoparticles present small coercive fields, about 1 kOe at 2 K (Figure 7), but the coercive field relative to the nanorods, when they are present in *in situ* samples, is quite high and comparable to that in the case of *ex situ* samples.

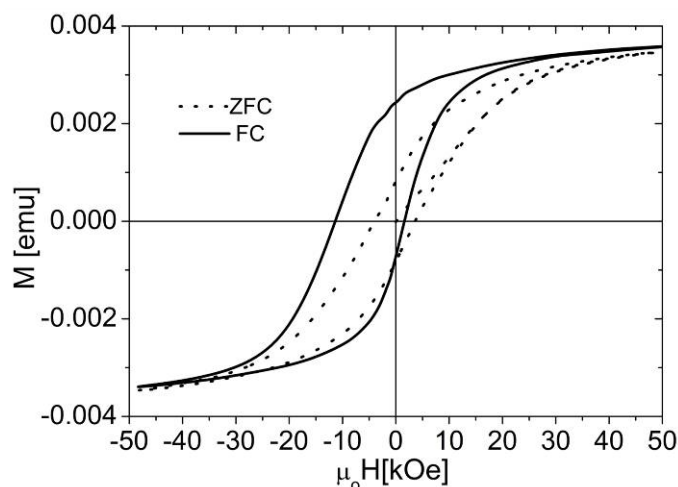
In both cases, when anisotropic nanoparticles are present, if the transition from the isotropic to the liquid crystal state is passed in the presence of the magnetic field, the magnetic properties are considerably improved

### 2.3. Liquid Crystal Elastomer Composite Synthesis

A first attempt in order to obtain a liquid crystal elastomer composite containing 1 wt% Co nanorods was performed by a two step hydrosilylation reaction in order first to substitute 75% of Si-H groups with the liquid crystal moiety 4'-(3-butenyloxy)phenyl-4-(methoxy)benzoate (M41) and then, after addition of 1 wt% 45 nm nanorods, to cross-link the polymer with a long chain aliphatic bridge. Our objective was to verify first of all the feasibility of the hydrosilylation reaction in the presence of the nanorods, and that the as-obtained elastomer was still a liquid crystal. The synthesis has been performed in air without taking any precaution against Co oxidation. The as-obtained elastomer possesses a liquid crystal to isotropic phase transition at 61 °C with a destabilization of 20 °C with respect to the elastomer without nanorods.

Hysteresis cycles were registered at 2 K after cooling down the sample without and with a 5 T magnetic field, they are presented in Figure 11. As expected the sample is oxidized, the cycle is not symmetric with respect to the zero magnetic field due to the presence of antiferromagnetic cobalt oxide, and the coercive field is low.

**Figure 11.** Hysteresis loops after Zero field Cooling (ZFC) and Field Cooling (FC,  $H = 5$  T) at 2 K for the elastomer doped with 1 wt% Co. Before the measurement the sample has been heated during 5 min at 400 K.



It is important to underline that the presence of Co nanorods did not inhibit the polymer cross-linking and a macroscopically homogeneous sample was obtained.

## 3. Experimental Section

### 3.1. Synthesis of the Samples

#### 3.1.1. In Situ Synthesis

The Co precursor, the liquid crystalline polymer, hexadecylamine (HDA, Fluka, 99%), and 4-(3-butenyloxy)benzoic acid (Boba) were dissolved separately in toluene ( $V_{\text{total}}$  from 12 to 16 mL) in a glove box, and then mixed under magnetic stirring. The resulting solution was put under a pressure

of 3 bars of hydrogen for 10 min. The solution was then heated at 120 °C during a time varying from 3 to 48 h. The black colloidal solution was removed from the heat source and cooled down under a cold water-jet to room temperature. The solvent was evaporated under vacuum.

For the synthesis in the presence of P41 different ratios Boba:Co and amine:Co were used, 0.15 and 1, corresponding to 10 wt% and 1.5 wt% of cobalt.

For the synthesis in the presence of P41Boba, Boba:Co = 1, 0.65 and 0.16 ratios corresponding to 0.8, 1.25 and 4.15 wt% of Co respectively; and Boba:HDA:Co = 0.16 :1:1 and 0.16:2:1 (4.15 wt% of Co) were used.

### 3.1.2. *Ex Situ* Synthesis

56 nm cobalt nanorods were suspended in toluene by sonication during 5 min and then added to a toluene polymer solution 150g/L; the final solution was sonicated again, left under mechanical stirring overnight and then the solvent was slowly evaporated under vacuum.

Due to the sensitivity of cobalt towards oxidation, all manipulations were performed in a glove box.

### 3.1.3. Liquid Crystal Elastomer

18.4 mg of polyhydrogenomethylsiloxane (Sigma Aldrich) were mixed to 68 mg of 4'-(3-butenyloxy)phenyl-4-(methoxy)benzoate (M41) in 1.5 mL toluene (Fisher Chemical, 99%), 100 µL of 0.06 wt% Karstedt catalyst (Platinum(0)-1,3-divinyl-1,1,3,3-tetramethyldisiloxane) solution was then added and the hydrosilylation reaction mixture was let for 1 hour at room temperature. A partially substituted liquid crystal polymer with 24% of free Si-H groups was so obtained. 1.23 mg 45 nm nanorods were dispersed in 500 µL of toluene and sonicated for 10 minutes. The polymer and nanorods solutions were mixed and the solvent partially evaporated before the addition of the cross-linking agent: 11.7 mg of docosadiene (Fluka) in 500 µL of toluene. The solvent was then slowly evaporated, and the solution sonicated for 25 min at the beginning of the solvent evaporation.

## 3.2. Analysis of the Samples

TEM characterizations were performed with a JEOL JEM 1011 microscope operating at 100 kV. TEM samples were prepared either on carbon coated grids by drop casting the reaction mixture before solvent evaporation (*in situ* samples) or by microtomy (*ex situ* samples). The thickness of the slices obtained by microtomy is about 70 nm. The transition temperatures of the final composite were characterized by Polarized Optical Microscopy, POM (Olympus BX50 microscope) in the case of the *in situ* synthesis and by Differential Scanning Calorimetry, DSC (Mettler Toledo DSC1 Star System) in the case of the *ex situ* synthesis. The values reported correspond to those determined from the position of the top of the peaks as the temperature decreased at a 10 °C/min rate.

The magnetic properties were analyzed by Superconducting Quantum Interference Device, SQUID (MPMS 5 QUANTUM DESIGN). The samples were introduced in gelatin capsules in order to prevent any oxidation, kept in a sealed schlenk, and rapidly transferred to the measurement cell. Samples were left at 400 K during 5 min in order to assure a random orientation of the nanorods at the beginning of the measurement.

#### 4. Conclusions

We have presented new composites obtained by mixing metallic cobalt particles and liquid crystal polymer matrices, either by an *in situ* synthesis of the particles or by an insertion of pre-formed particles inside the mesomorphous polymer. Even if nanoparticle dispersions were not perfectly homogeneous in the second case, mixing preformed metallic cobalt nanorods in the polymer matrix allowed us to introduce well-defined particles in the polymer.

All these materials present both mesomorphous and ferromagnetic properties. The liquid crystalline order is maintained in the presence of the nanorods at least up to 5 wt% of cobalt. The magnetic properties are improved compared to the properties of the same nanorods in an inert matrix.

The realization of a first tridimensional composite validates the possibility to synthesize ferromagnetic liquid crystalline elastomers.

Coupling the inherent advantages of magnetic nanoparticles and liquid crystal groups could result in materials with interesting magnetic properties and orientational behavior, while providing simultaneously mechanical properties, which are mandatory for applications such as actuators.

#### Acknowledgments

The authors thank European training site (Nanotool), ANR Agency (MaCriLiMa JC&JC2010), the EU (FEDER-35477 “Nano-objets pour la biotechnologie”) for financial support; TEMSCAN service for TEM measuring time, Isabelle Fourquaux and CMEAB for microtomy of *in situ* samples and A. Mari for SQUID measurements.

#### References

1. Behl, M.; Lendlein, A. Shape-memory polymers. *Mater. Today* **2007**, *10*, 20–28.
2. De Gennes, P.-G. Possibilités offertes par la reticulation de polymeres en presence d'un cristal liquide. *Phys. Lett.* **1969**, *28*, 725–726.
3. Küpfer, J.; Finkelmann, H. Nematic liquid single crystal elastomers. *Makromol. Chem. Rapid Commun.* **1991**, *12*, 717–726.
4. Burke, K.A.; Mather, P.T. Soft shape memory in main-chain liquid crystalline elastomers. *J. Mater. Chem.* **2010**, *20*, 3449–3457.
5. Kondo, M.; Yu, Y.; Ikeda, T. How does the initial alignment of mesogens affect the photoinduced bending behavior of liquid-crystalline elastomers? *Angew. Chem. Int. Ed.* **2006**, *45*, 1378–1382.
6. Lehmann, W.; Skupin, H.; Toiksdorf, C.; Gebhard, E.; Zentel, R.; Kruger, P.; Losche, M.; Kremer, F. Giant lateral electrostriction in ferroelectric liquid-crystalline elastomers. *Nature* **2001**, *410*, 447–450.
7. Brochard, F.; de Gennes, P.G. Theory of magnetic suspensions in liquid crystals. *J. Phys. (Paris)* **1970**, *31*, 691–708.
8. Chen, S.-H.; Amer, N.M. Observation of macroscopic collective behavior and new texture in magnetically doped liquid crystals. *Phys. Rev. Lett.* **1983**, *51*, 2298–2301.
9. Neto, A.M.F.; Saba, M.M.F. Determination of the minimum concentration of ferrofluid required to orient nematic liquid-crystals. *Phys. Rev. A* **1986**, *34*, 3483–3485.

10. Martinez-Miranda, L.J.; Kurihara, L.K. Interaction and response of a smectic-A liquid crystal to a nanometer particle: Phase transition due to the combined effect of the functionalization compound and particle size. *J. Appl. Phys.* **2009**, *105*, No. 084305.
11. Da Cruz, C.; Sandre, O.; Cabuil, V. Phase behavior of nanoparticles in a thermotropic liquid crystal. *J. Phys. Chem. B* **2005**, *109*, 14292–14299.
12. Song, H.M.; Kim, J.C.; Hong, J.H.; Lee, Y.B.; Choi, J.; Lee, J.I.; Kim, W.S.; Kim, J.H.; Hur, N.H.; Magnetic and transparent composites by linking liquid crystals to ferrite nanoparticles through covalent networks. *Adv. Funct. Mater.* **2007**, *17*, 2070–2076.
13. Kaiser, A.; Winkler, M.; Krause, S.; Finkelmann, H.; Schmidt, A.M. Magnetoactive liquid crystal elastomer nanocomposites. *J. Mater. Chem.* **2009**, *19*, 538–543.
14. Garcia-Marquez, A.; Demortière, A.; Heinrich, B.; Guillon, D.; Bégin-Colin, S.; Donnio, B. Iron oxide nanoparticle-containing main-chain liquid crystalline elastomer: Towards soft magnetoactive networks. *J. Mater. Chem.* **2011**, *21*, 8994–8996.
15. Zadoina, L.; Lonetti, B.; Soulantica, K.; Mingotaud, A.F.; Respaud, M.; Chaudret, B.; Mauzac, M. Liquid crystalline magnetic materials. *J. Mater. Chem.* **2009**, *19*, 8075–8078.
16. Zadoina, L.; Soulantica, K.; Ferrere, S.; Lonetti, B.; Respaud, M.; Mingotaud, A.F.; Falqui, A.; Genovese, A.; Chaudret, B.; Mauzac, M. *In situ* synthesis of cobalt nanoparticles in functionalized liquid crystalline polymers. *J. Mater. Chem.* **2011**, *21*, 6988–6994.
17. Palaprat, G.; Mingotaud, A.F.; Langevin, D.; Marty J.D.; Mauzac, M. Sorption properties of functionalized liquid crystalline networks. *J. Phys. Chem. B* **2008**, *112*, 6603–6608.
18. Andersen, R.A.; Faegri, K.; Green, J.C.; Haaland, A.; Lappert, M.F. Leung, W.P.; Rypdal, K. Synthesis of bis[bis(trimethylsilyl)amido]iron(II). Structure and bonding in  $M[N(\text{SiMe}_3)_2]_2$  (M = manganese, iron, cobalt): Two-coordinate transition-metal amides. *Inorg. Chem.* **1988**, *27*, 1782–1786.
19. Wetz, F.; Soulantica, K.; Respaud, M.; Falqui, A.; Chaudret, B. Synthesis and magnetic properties of Co nanorod superlattices. *Mater. Sci. Eng. C* **2007**, *27*, 1162–1166.
20. Mitov, M.; Portet, C.; Bourgerette, C.; Snoeck, E.; Verelst, M. Long-range structuring of nanoparticles by mimicry of a cholesteric liquid-crystal. *Nat. Mater.* **2002**, *1*, 229–231.
21. Saliba, S.; Coppel, Y.; Davidson, P.; Mingotaud, C.; Chaudret, B.; Kahn, M.L.; Marty, J.D. Liquid crystal based on hybrid zinc oxide nanoparticles. *J. Mater. Chem.* **2011**, *21*, 6821–6823.